Int. J. Non-Linear Mechanics. Vol. 12, pp. 91–101. Pergamon Press 1977. Printed in Great Britain

EQUILIBRIUM AND STABILITY OF A WHIRLING ROD-MASS SYSTEM

J. J. RUSSELL and W. J. ANDERSON
United States Air Force Academy, CO 80840, U.S.A.
and
The University of Michigan, Ann Arbor, MI 48105, U.S.A.

(*Received* 20 *August* 1976)

Abstract—A two-degree-of-freedom lumped-mass model is used to gain understanding of the equilibrium and stability of a circularly towed cable. Particular cases considered are those of no drag, viscous drag, and viscous drag with a crosswind.

1. INTRODUCTION

The problem of the equilibrium shape of a circularly towed cable has been of interest for several centuries. The linear eigenvalue problem for a cable spun in a vacuum about its own axis (zero tow radius) was first studied by D. Bernoulli (1700–1782) and L. Euler (1707–1783). The problem was then abandoned until 1955 when Kolodner [1] studied the non-linear eigenvalue problem. The first attempt to study the non-linear forced response (nonzero tow radius) was by Caughey [2]. Since then there have been many investigators, including the present authors [3], who have used various numerical methods to obtain solutions to the continuous system using specific values of the governing parameters. Very little progress has been made toward understanding the general behavior of this system.

The present work is a portion of an overall effort [4] which successfully employed the finite element method to obtain solutions to the problem of a continuous whirling cable subjected to aerodynamic drag. Because of the highly non-linear nature of the problem, *a priori* knowledge of the nature of the solutions is necessary. This study provided the information and predicted other phenomena which could occur and might not otherwise have been found in a purely numerical study.

To gain insight into this complex system, the simplest model exhibiting the qualitative behavior of the actual system is examined. This model is an inextensible massless rod with a lumped mass attached at the tip. The geometry and associated coordinate systems are shown in Fig. 1.

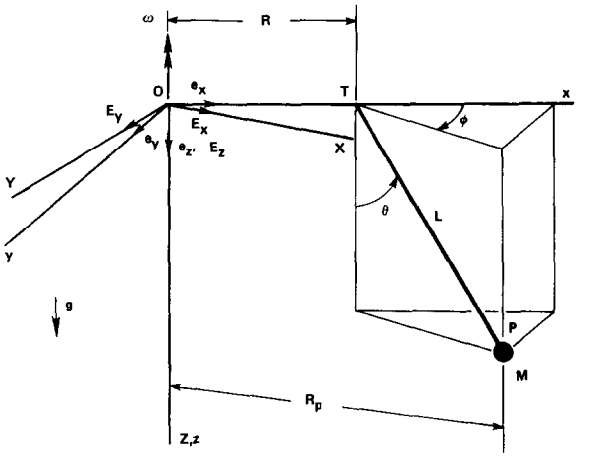

Fig. 1. Single lumped mass system.

The non-linear eigenvalue and response equilibrium positions for the case of a vacuum are found and their stability determined using the perturbed equations of motion. A viscous drag law is then utilized to examine the effects of drag without introducing the complexity of aerodynamic drag. Once more equilibrium positions are found and their stability determined. A linearized model is then employed to investigate the effects of a crosswind on the motion of the model.

2. EQUATIONS OF MOTION

The XYZ cartesian coordinate system is an inertial reference system, while the xyz coordinate system rotates with an angular velocity ω about the z axis. The mass M is attached to a massless-inextensible rod of length L which is in turn attached to the tow point T with a frictionless ball-joint connection. The tow point is a distance R along the x axis. The angular velocity ω of the tow bar $\overline{OT}$ is constant. The elevation angle θ and lag angle ϕ are generalized coordinates describing the position of the tip mass.

External forces acting on the system are gravity, directed in the $\mathbf{E}_z$ direction, and viscous drag on the sphere. The drag force is proportional to the magnitude of the velocity of the sphere relative to the fluid and is directed opposite to the relative velocity. The relative velocity, $\mathbf{v}_r$ is the vector difference of the absolute velocities of the tip mass and crosswind, hence the viscous drag force $\mathbf{F}_d$ is given by

$$\mathbf{F}_d = -c\mathbf{v}_r \tag{2.1}$$

where c is the viscous drag coefficient. If the crosswind is assumed to have a constant magnitude v_w and to have a constant direction α (where α is the angle the wind vector makes with the X axis and is positive by the right hand rule about the positive Y axis), the nondimensional equations of motion are obtained from Lagrange's equation as

$$\begin{aligned}
&\Omega^2[\ddot{\theta}-\varepsilon\cos\theta\cos\phi-(\dot{\phi}-1)^2\sin\theta\cos\theta]+\Omega\zeta[\dot{\theta}-\varepsilon\cos\theta\sin\phi]\\
&\quad+\sin\theta=-\beta[\cos\alpha\cos\theta\cos(\tau-\phi)-\sin\alpha\sin\theta]\\
&\Omega^2[\sin^2\theta\ddot{\phi}+2(\dot{\phi}-1)\dot{\theta}\sin\theta\cos\theta+\varepsilon\sin\theta\sin\phi]\\
&\quad+\Omega\zeta[(\dot{\phi}-1)\sin^2\theta-\varepsilon\sin\theta\cos\phi]=-\beta\cos\alpha\sin\theta\sin(\tau+\phi)
\end{aligned} \tag{2.2}$$

where $(\dot{\ }) = \mathrm{d}(\ )/\mathrm{d}\tau$ and the following parameters have been defined:

Ω, the nondimensional rotational velocity

$$\Omega = \omega\sqrt{\frac{L}{g}} \tag{2.3a}$$

ε, the nondimensional tow radius

$$\varepsilon = \frac{R}{L} \tag{2.3b}$$

ζ, the nondimensional drag coefficient

$$\zeta = \frac{c}{M}\sqrt{\frac{L}{g}} \tag{2.3c}$$

β, the nondimensional crosswind coefficient

$$\beta = \frac{cv_w}{Mg} \tag{2.3d}$$

τ, the nondimensional time

$$\tau = \omega t\,. \tag{2.3e}$$

The equilibrium equations may then be obtained from (2.2) by setting the time derivatives and wind coefficient β equal to zero, yielding

$$\begin{aligned}
&\sin\theta_0(1-\Omega^2\cos\theta_0)-\Omega^2\varepsilon\cos\theta_0\cos\phi_0-\Omega\zeta\varepsilon\cos\theta_0\sin\phi_0=0\\
&\zeta(\sin\theta_0+\varepsilon\cos\phi_0)-\Omega\varepsilon\sin\phi_0=0
\end{aligned} \tag{2.4}$$

where θ_0 and ϕ_0 are the equilibrium values of θ and ϕ respectively.

A convenient variable which characterizes the behavior of the system is the non-dimensional tip radius r_p defined as R_p/L.

$$r_p = (\varepsilon^2 + 2\varepsilon \sin\theta_0 \cos\phi_0 + \sin^2\theta_0)^{1/2}. \tag{2.5}$$

This variable allows construction of amplitude r_p vs frequency Ω plots as in vibration problems.

The stability of an equilibrium position must be determined using a dynamic stability criterion since the system is nonconservative. Perturbing the equations of motion (2.2) about the equilibrium values θ_0 and ϕ_0 yields linearized equations of motion in the neighborhood of the equilibrium position.

$$[M]\{\ddot{\xi}\} + [C]\{\dot{\xi}\} + [K]\{\xi\} = \{0\} \tag{2.6}$$

where $\{\xi\}$ is the column vector of the perturbed coordinates. The inertial matrix $[M]$ is given by

$$[M] = \Omega^2 \begin{bmatrix} 1 & 0 \\ 0 & \sin^2\theta_0 \end{bmatrix} \tag{2.7}$$

while the "damping" matrix is

$$[C] = \begin{bmatrix} \Omega\zeta & \Omega^2 \sin 2\theta_0 \\ -\Omega^2 \sin 2\theta_0 & \Omega\zeta \sin^2\theta_0 \end{bmatrix} \tag{2.8}$$

and the stiffness matrix is

$$[K] = \begin{bmatrix} k_{11} & k_{12} \\ k_{21} & k_{22} \end{bmatrix} \tag{2.9}$$

where

$$\begin{aligned}
k_{11} &= \Omega^2[\varepsilon \sin\theta_0 \cos\phi_0 - \cos 2\theta_0] + \Omega\zeta\varepsilon \sin\theta_0 \sin\phi_0 + \cos\theta_0 \\
&\quad - \beta[\cos\alpha \sin\theta_0 \cos(\tau - \phi_0) + \sin\alpha \cos\theta_0] \\
k_{12} &= \varepsilon[\Omega^2 \cos\theta_0 \sin\phi_0 - \Omega\zeta \cos\theta_0 \cos\phi_0 + \beta \cos\alpha \cos\theta_0 \sin(\tau - \phi)] \\
k_{21} &= \varepsilon[\Omega^2 \cos\theta_0 \sin\phi_0 - \Omega\zeta \cos\theta_0 \cos\phi_0] - \Omega\zeta \sin 2\theta_0 + \beta \cos\alpha \cos\theta_0 \sin(\tau + \phi_0) \\
k_{22} &= \varepsilon\Omega^2 \sin\theta_0 \cos\phi_0 + \Omega\zeta\varepsilon \sin\theta_0 \sin\phi_0 + \beta \cos\alpha \sin\theta_0 \cos(\tau + \phi_0).
\end{aligned} \tag{2.10}$$

The coefficient matrices $[M]$, $[C]$, and $[K]$ reveal a great deal about the nature of the stability problem. The inertial matrix $[M]$ is diagonal, symmetric, and positive definite for all θ_0, as expected.

The "damping" matrix $[C]$ can be decomposed into a symmetric dissipative damping matrix $[C_v]$ and a skew-symmetric gyroscopic matrix $[C_g]$, where

$$\begin{aligned}
[C_v] &= \Omega\zeta \begin{bmatrix} 1 & 0 \\ 0 & \sin^2\theta_0 \end{bmatrix} \\
[C_g] &= \Omega^2 \sin 2\theta_0 \begin{bmatrix} 0 & 1 \\ -1 & 0 \end{bmatrix}.
\end{aligned} \tag{2.11}$$

The decomposition of the stiffness matrix $[K]$ also contains skew symmetric terms due to the nonconservative position-dependent forces created by drag and wind. The stiffness matrix also has elements which are periodic in time due to the crosswind, thus creating a coupled pair of Hill equations containing damping, gyroscopic, and nonconservative effects.

Bolotin [5] has shown for a nonconservative system that a diagonal damping matrix is destabilizing for slight damping when the diagonal elements of the dissipative damping matrix are not equal. However, for sufficiently large values of the drag coefficient ζ, damping can once more have a stabilizing effect.

The problem at hand, neglecting wind, adds two important features: (1) a possible stabilizing effect due to gyroscopic forces, and (2) a destabilizing effect due to the nonconservative forces which vary linearly with the drag coefficient. Thus, nonconservative drag forces can cancel the stabilizing effects of the damping matrix for even large values of ζ.

Assuming exponential motion

$$\{\xi\} = \{\Xi\}\, e^{\lambda\tau} \tag{2.12}$$

leads to the eigenvalue problem

$$|\lambda^2[M]+\lambda[C]+[K]| = 0 \tag{2.13}$$

which upon expansion yields

$$p_0\lambda^4+p_1\lambda^3+p_2\lambda^2+p_3\lambda+p_4 = 0 \tag{2.14}$$

where

$$\begin{aligned} p_0 &= \Omega^4 \sin^2\theta_0 \\ p_1 &= 2\Omega^3\zeta \sin^2\theta_0 \\ p_2 &= \Omega^2[\zeta^2 \sin^2\theta_0+\Omega^2 \sin^2 2\theta_0+(k_{11}\sin^2\theta_0+k_{22})] \\ p_3 &= \Omega\zeta[(k_{11}\sin^2\theta_0+k_{22})+\Omega^2\sin^2 2\theta_0] \\ p_4 &= k_{11}k_{22}-k_{12}k_{21}. \end{aligned} \tag{2.15}$$

Rather than solving for the roots of (2.14). it is advantageous to use the Routh–Hurwitz criteria when drag is present. These criteria state that necessary and sufficient conditions for asymptotic stability are

$$p_1 > 0 \tag{2.16a}$$

$$p_1p_2-p_0p_3 > 0 \tag{2.16b}$$

$$(p_1p_2-p_0p_3)p_3-p_1^2p_4 > 0 \tag{2.16c}$$

$$p_4 > 0. \tag{2.16d}$$

Note that the static instability ($\lambda = 0$) is given when the fourth condition is violated, i.e. $p_4 \leqslant 0$. As long as drag exists $p_1 > 0$, hence conditions (b) and (c) represent dynamic stability criteria.

In the case of no drag ($\zeta = 0$) only orbital stability can be shown and (2.14) can be used directly since $p_1 = p_3 = 0$ thus reducing it to a quadratic in λ^2.

The equilibrium and stability of the system with and without viscous drag as well as the behavior of the system with wind are now considered.

3. THE RESPONSE PROBLEM IN A VACUUM

Solving the equilibrium equations (2.4) for the case of no drag yields

$$\phi_0 = 0 \quad \text{or} \quad \phi_0 = \pi \tag{3.1}$$

and

$$\sin\theta_0(1-\Omega^2\cos\theta_0) = \pm\varepsilon\Omega^2\cos\theta_0 \tag{3.2}$$

where $+\varepsilon$ corresponds to $\phi_0 = 0$ and $-\varepsilon$ to $\phi_0 = \pi$.

The non-linear eigenvalue problem obtained by setting $\varepsilon = 0$ in (3.2) is found in many texts (See Greenwood [6]) and will not be covered here.

From (3.2), the solution to the response problem ($\varepsilon \neq 0$) may be written in the form

$$\Omega^2 = \frac{\tan\theta_0}{\sin\theta_0 \pm \varepsilon}. \tag{3.3}$$

Bearing in mind that this model is used to represent a cable, only solutions to (3.3) below the tow plane are considered. From (3.3), equilibrium solutions for which Ω is real exist only for θ in the ranges $(0, \pi/2)$ for $\phi_0 = 0$ and $(\sin^{-1}\varepsilon, \pi/2)$ for $\phi_0 = \pi$. The out-of-phase solution $\phi_0 = \pi$ does not exist for $\varepsilon > 1$ since the tow radius is greater than the rod length thus making it impossible for the mass to cross the spin axis. Amplitude-frequency plots using (3.3) and (2.5) for $\varepsilon = 0.1$ and $\varepsilon = 0.3$ are shown in Fig. 2. These plots are very similar to those obtained for the forced response, amplitude vs driving frequency plots for a mass-hardening spring system with no damping.

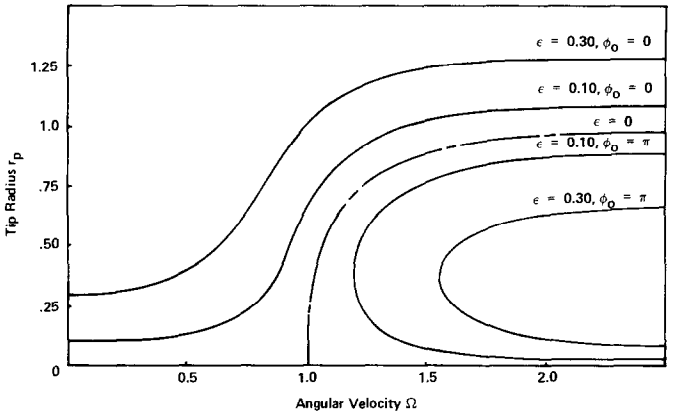

Fig. 2. Tip radius vs angular velocity for non-linear response in vacuum.

Once all drag-dependent terms are set to zero the stiffness matrix is symmetric and the "damping" matrix is purely gyroscopic. This problem has the same form then as that of a rotating shaft problem with no damping. One important difference exists in that the stiffness of the shaft is always positive while the "stiffnesses" of the rotating bar are geometry dependent and can be negative. Setting $\zeta = 0$ and dividing (2.14) through by p_0 yields the characteristic equation

$$\lambda^4 + [\omega_1^2 + \omega_2^2 + \delta^2]\lambda^2 + \omega_1^2\omega_2^2 = 0 \tag{3.4}$$

where

$$\omega_1^2 = \frac{\sin^3\theta_0 \pm \varepsilon}{\sin\theta_0} \qquad \omega_2^2 = \frac{\pm\varepsilon}{\sin\theta_0} \qquad \delta^2 = 4\cos^2\theta_0 . \tag{3.5}$$

The dependence on Ω^2 has been removed by using the equilibrium equation (3.3). The characteristic equation is easily solved for λ^2 and the following stability criteria obtained, i.e. the solution is orbitally stable if and only if

$$\omega_1^2\omega_2^2 > 0 \tag{3.6a}$$

$$\omega_1^2 + \omega_2^2 + \delta^2 > 0 \tag{3.6b}$$

$$(\omega_1^2 + \omega_2^2 + \delta^2)^2 - 4\omega_1^2\omega_2^2 > 0 \tag{3.6c}$$

holds simultaneously.

Conditions (3.6a) and (3.6b) represent static stability criteria while condition (3.6c) represents a dynamic stability criterion. It is instructive to suppress the role of the driving frequency and view the problem in terms of geometrical variables. The conditions (3.6) can be rewritten in terms of the equilibrium elevation angle θ_0 and the tow radius using (3.5). The criteria of (3.6) then become

$$\varepsilon \pm \sin^3\theta_0 > 0 \tag{3.7a}$$

$$4\sin\theta_0 - 3\sin^3\theta_0 \pm 2\varepsilon > 0 \tag{3.7b}$$

$$\sin^4\theta_0 + 8\sin^2\theta_0\cos^2\theta_0 + 16\cos^4\theta_0 \pm 16\varepsilon\frac{\cos^2\theta_0}{\sin\theta_0} > 0 . \tag{3.7c}$$

For the case of the in-phase solution $\phi_0 = 0$, conditions (3.7) are satisfied for all θ_0, hence all in-phase equilibrium solutions are orbitally stable. Rewriting the stability criteria for the out-of-phase solution $\phi_0 = \pi$ and solving for ε yields

$$\varepsilon > \sin^3\theta_0 \tag{3.8a}$$

$$\varepsilon < \tfrac{1}{2}(4\sin\theta_0 - 3\sin^3\theta_0) \tag{3.8b}$$

$$\varepsilon < \frac{1}{16}\frac{\sin\theta_0}{\cos^2\theta_0}[3\cos^2\theta_0 + 1]^2 . \tag{3.8c}$$

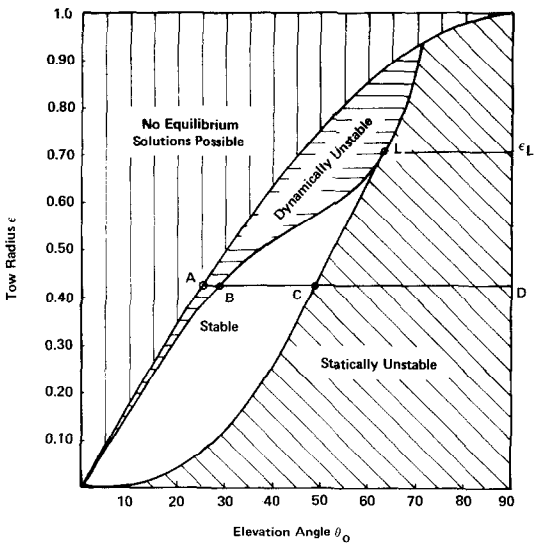

Fig. 3. Stability diagram in the $\varepsilon - \theta_0$ plane for the out of phase solution, $\phi_0 = \pi$.

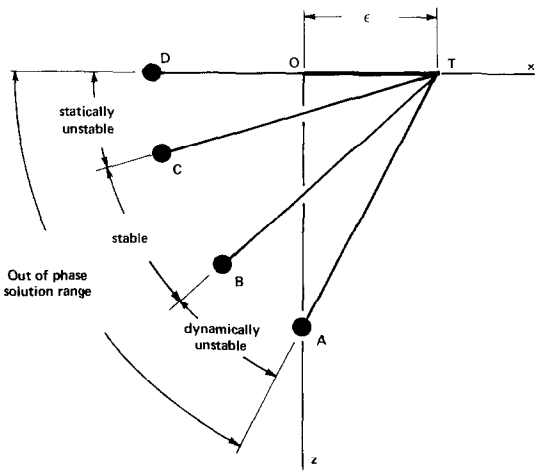

Fig. 4. Stability diagram for out of phase equilibrium positions.

The relevant stability boundaries using (3.8) are shown in Fig. 3. Stable out-of-phase solutions exist only for $\varepsilon < \varepsilon_L$ where ε_L is the common intersection of all the criteria of (3.8) and is given by

$$\varepsilon_L = (4/5)^{3/2} = 0.7155. \tag{3.9}$$

These results can be interpreted in terms of the frequency by referring to Figs. 3 and 4 and considering $\varepsilon < \varepsilon_L$. As the mass moves from position A (asymptotic solution $r_p = 0$ for $\Omega^2 \to \infty$) to position D (asymptotic solution $r_p = 1 - \varepsilon$ for $\Omega^2 \to \infty$), a dynamically unstable region AB is passed through first, then a stable region BC, and then a statically unstable region CD. It can easily be shown that the static stability criterion (3.8a) coincides with the "vertical tangency" point of the out-of-phase solution of the frequency-response curve. An equilibrium stability plot for $\varepsilon = 0.45$ is shown in Fig. 5.

The eigenvalues obtained from (3.4) could be used to generate eigenvectors in the standard manner. But since the only question was one of stability, that will not be done here. However, it is interesting to note that when it is done, the resulting motions are uncoupled in the case of the static instability, but coupled through gyroscopic effects for the dynamic instability. Therefore, even though the equilibrium solutions lie in the $\phi_0 = 0, \pi$ plane, the perturbed motion does not; and any stability analysis which attempted to treat the system as a single degree-of-freedom system would fail.

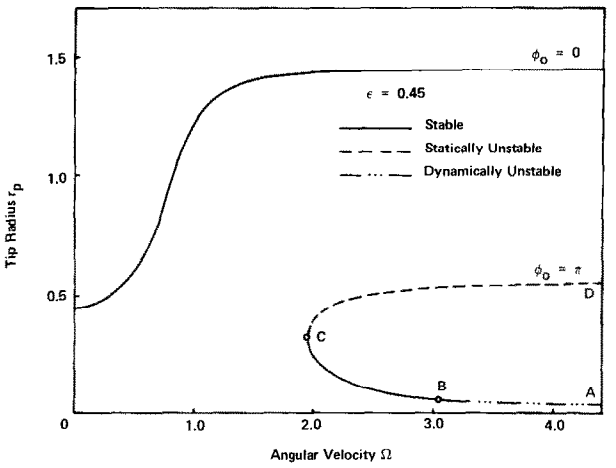

Fig. 5. Stability of equilibrium for non-linear response in a vacuum.

If the gyroscopic effects are neglected, it can be shown that the out-of-phase solution is always statically unstable; therefore, by adding these effects a portion of the lower branch of the curve is stable and the nature of the instability is changed from static to dynamic for the remainder.

Once again the analogy between the response of the rotating pendulum and the forced response of the hardening spring-mass system described by Duffing's equation is evident. The amplitude-frequency plots and static instabilities are very similar, but two new features are added by the rotating pendulum. The first is that of a "cut off" value ($\varepsilon \geqslant 1$) of the forcing mechanism for which the out-of-phase solution disappears. The second is that of the dynamic instability caused by the interaction of gyroscopic and negative geometric stiffness effects.

4. THE RESPONSE PROBLEM WITH VISCOUS DRAG

The effects of viscous drag will now be considered by solving the equilibrium equations for $\zeta \neq 0$ and $\varepsilon \neq 0$. These equations are coupled transcendental equations and would be, in general, very difficult to solve. Solutions can be obtained, however, by noting that the system is linear in $\sin\phi_0$ and $\cos\phi_0$. Solving (2.4) as a set of nonhomogeneous linear algebraic equations in the unknowns $\sin\phi_0$ and $\cos\phi_0$ yields

$$\sin\phi_0 = \frac{\zeta\tan\theta_0}{\Omega\varepsilon(\Omega^2+\zeta^2)}$$
$$\cos\phi_0 = \frac{\tan\theta_0-(\Omega^2+\zeta^2)\sin\theta_0}{\varepsilon(\Omega^2+\zeta^2)}. \tag{4.1}$$

The phase angle ϕ_0 can be eliminated using

$$\cos^2\phi_0+\sin^2\phi_0 = 1 \tag{4.2}$$

thus giving a quadratic equation in Ω^2

$$[\cos^2\theta_0(\sin^2\theta_0-\varepsilon^2)]\Omega^4+[\zeta^2(\sin^2\theta_0-\varepsilon^2)\cos^2\theta_0 - 2\sin^2\theta_0\cos\theta_0]\Omega^2+\sin^2\theta_0 = 0. \tag{4.3}$$

The solution to this equation is

$$\Omega^2 = \frac{-B\pm\sqrt{B^2-4AC}}{2A} \quad A\neq 0 \tag{4.4}$$

where

$$A = (\sin^2\theta_0-\varepsilon^2)\cos^2\theta_0$$
$$B = \zeta^2A-2\sin^2\theta_0\cos\theta_0 \tag{4.5}$$
$$C = \sin^2\theta_0.$$

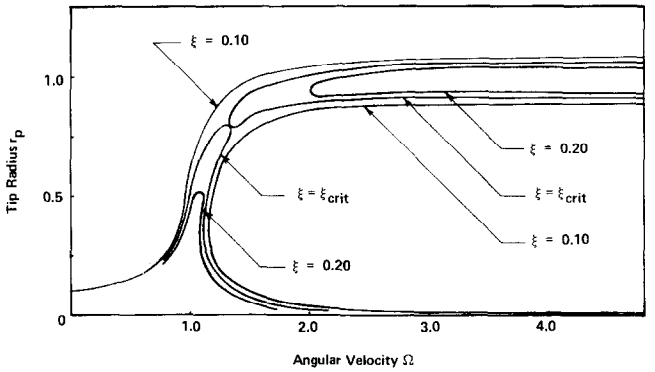

Fig. 6. Tip radius vs angular velocity for non-linear response with viscous drag.

Once again it can be shown that only one solution branch exists for $\varepsilon \geqslant 1$; therefore, the case of $\varepsilon < 1$ will be the one studied in detail.

The amplitude-frequency plot shown in Fig. 6 was constructed using the equilibrium equation (4.4) and the definition of the tip radius (2.5). If ζ is chosen such that it is slightly greater than zero, the curve does not change qualitatively from the case of zero drag. This differs from the damped hardening-spring analogy in that if a slight amount of damping is added, the in-phase and out-of-phase solutions merge and the resulting vertical tangency point moves in from $\Omega = \infty$ as the damping is increased.

As ζ is increased the in-phase and out-of-phase solutions neck down until at a critical value of ζ a separatrix is formed. As ζ is increased still further the two branches break apart. At high values of damping ζ, the low-amplitude portion of the in-phase solution is joined to the low-amplitude portion of the out-of-phase solution. The corresponding large amplitude solutions of the in- and out-of-phase solutions form the separated upper branch.

Stability of the equilibrium solutions as determined from the Routh–Hurwitz criteria (2.16) is shown in the amplitude-frequency plot of Fig. 7 for $\varepsilon = 0.1$ and $\zeta = 0.10$ and $\zeta = 0.165$. An analysis of the asymptotic positions (1) $\theta_0 = \pi/2$, $\phi_0 = 0$, (2) $\theta_0 = \pi/2$, $\phi_0 = \pi$, and (3) $\theta_0 = \sin^{-1}\varepsilon$, $\phi_0 = \pi$ shows that position (1) is stable, (2) is statically unstable, and (3) is dynamically unstable regardless of the values of ε or ζ.

Therefore, from Fig. 7 the effects of viscous drag are most dramatic for $\zeta > \zeta_{crit}$. If ζ is close to ζ_{crit}, the system has the possibility of three non-linear jumps. The first occurs at A where the system jumps from the large tip radius solution at A to the small amplitude solution at B as Ω is increased. If Ω is now decreased, a second jump will occur at C where the jump will be from a small tip radius to a larger one at D. If the bar can be made to assume a position on the stable portion of the upper branch and Ω then decreased, a jump will occur at E from a large tip radius to a small one at F. These jump instabilities are static in nature. The dynamic instability boundary does not appear in Fig. 7 since the small value of ε necessary to illustrate the jump phenomena causes the dynamic instability boundary to appear only at extremely large values of Ω.

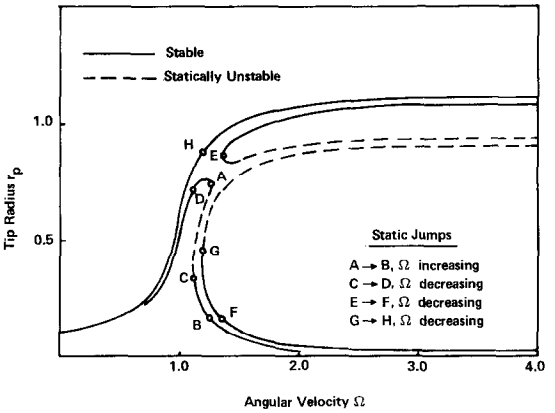

Fig. 7. Stability of equilibrium for non-linear response with viscous drag.

5. CROSSWIND EFFECTS

The effects of crosswind for small crosswind coefficients β, are investigated by considering the perturbed equations of motion (2.6). These are first simplified to the case of a horizontal crosswind $\alpha = 0$. The stiffness coefficients are:

$$\begin{aligned}
k_{11} &= \Omega^2[\varepsilon \sin\theta_0 \cos\phi_0 - \cos 2\theta_0] + \Omega\zeta\varepsilon \sin\theta_0 \sin\phi_0 + \cos\theta_0 - \beta \sin\theta_0 \cos(\tau - \phi_0) \\
k_{12} &= \varepsilon[\Omega^2 \cos\theta_0 \sin\phi_0 - \Omega\zeta \cos\theta_0 \cos\phi_0] + \beta \cos\theta_0 \sin(\tau - \phi_0) \\
k_{21} &= \varepsilon[\Omega^2 \cos\theta_0 \sin\phi_0 - \Omega\zeta \cos\theta_0 \cos\phi_0] - \Omega\zeta \sin 2\theta_0 + \beta \cos\theta_0 \sin(\tau + \phi_0) \\
k_{22} &= \varepsilon\Omega^2 \sin\theta_0 \cos\phi_0 + \Omega\zeta\varepsilon \sin\theta_0 \sin\phi_0 + \beta \sin\theta_0 \cos(\tau + \phi_0).
\end{aligned} \tag{5.1}$$

Even with this simplification, the motion is described by a coupled pair of Hill equations. Therefore, to simplify even further, the perturbed ϕ motion is constrained such that $\phi_0 = 0$. The elevation angle θ_0 is correspondingly redefined such that $(-\pi/2 < \theta_0 < \pi/2)$. The θ perturbed equation of motion is

$$\ddot{\Theta} + \hat{c}\dot{\Theta} + \hat{k}\Theta = 0 \tag{5.2}$$

where

$$\begin{aligned}
\hat{c} &= \zeta/\Omega \\
\hat{k} &= [\varepsilon \sin\theta_0 - \cos 2\theta_0] + \frac{\cos\theta_0}{\Omega^2} - \beta \cos\tau
\end{aligned} \tag{5.3}$$

and

$$\hat{\beta} = \frac{\beta \sin\theta_0}{\Omega^2}.$$

The expressions for $\hat{k}$ and $\hat{\beta}$ are next written as a function of θ_0 using the equilibrium equation (3.2).

$$\begin{aligned}
\hat{k} &= \omega_1^2 - \beta \cos\tau \\
\hat{\beta} &= \beta \cos\theta_0(\sin\theta_0 + \varepsilon)
\end{aligned} \tag{5.4}$$

where ω_1^2 was defined previously as

$$\omega_1^2 = \frac{\sin^3\theta_0 + \varepsilon}{\sin\theta_0}. \tag{5.5}$$

Substitution of $\hat{k}$ (5.4) into (5.2) yields

$$\ddot{\Theta} + \hat{c}\dot{\Theta} + (\omega_1^2 - \hat{\beta}\cos\tau)\Theta = 0 \tag{5.6}$$

which is a damped Mathieu equation. Bolotin [5] has shown that the Strutt diagram for the undamped Mathieu is modified by damping as shown in Fig. 8.

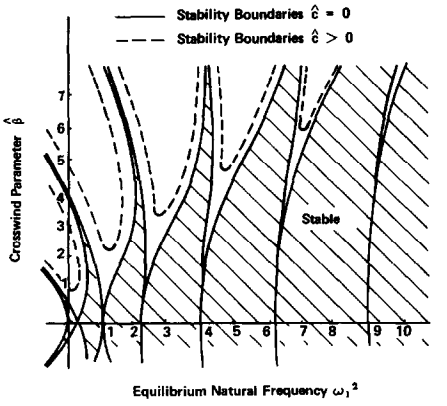

Fig. 8. Stability diagram for the constrained system with crosswind.

Therefore, as long as $\omega_1^2 > 0$ (which is the case for $0 \geqslant \theta_0 \leqslant \pi/2$) the system is stable for no crosswind. This is in agreement with the results of Section 2. It is clear from Fig. 8 that for a given equilibrium position there is a value of the crosswind velocity parameter $\hat{\beta}$ which will cause unstable motion.

Generalization from the results of the out-of-phase solution for the more complex system should not be made from this highly simplified model, because the single degree-of-freedom assumption eliminates the possibility of Coriolis stabilization. Therefore, the resulting interaction with the negative stiffnesses which cause the dynamic instability could not occur.

Thus it has been shown that even under simplifying assumptions, the rotating rod-mass system with crosswind results in a problem of parametric excitation dependent both on the magnitude of the crosswind velocity and the angular velocity of the system.

6. CONCLUSION

This study has considered the simplest model which will illustrate the qualitative behavior of a circularly towed cable, that of an inextensible massless rod with an attached tip mass. Equilibrium positions in the rotating reference frame were found and plotted using tip amplitude-frequency plots for the cases of no drag and viscous drag. The analogies between these plots and those for a hardening-spring system with and without damping were shown. A new feature not present in the damped hardening-spring system, the detached upper branch, was shown to exist.

Stability of the equilibrium solutions was determined using the perturbed equations of motion. A dynamic instability in the out-of-phase solution was found for the case of no drag. This instability was dynamic in nature even though nonconservative forces were not present and is caused by an interaction of stabilizing effects due to gyroscopic terms and destabilizing effects due to centripetal acceleration terms. Addition of viscous drag further complicates the stability by adding dissipative damping and nonconservative stiffness. Neither can be considered separately since both are linearly dependent on the drag coefficient. Both of these effects may cause further destabilization depending on the amount of drag present.

The presence of dynamic instabilities caused by wind-induced parametric excitation was demonstrated even after very restrictive simplifying assumptions were made.

REFERENCES

1. I. I. Kolodner, Heavy rotating string—a non-linear eigenvalue problem. In *Communications on Pure and Applied Mathematics*, Vol. VIII, 395–408 (1955).
2. T. K. Caughey, Whirling of a heavy chain, *Proc. 3rd U.S. National Congress of Applied Mechanics*, 61–108 (1958).
3. J. J. Russell and W. J. Anderson, Whirling cable subjected to viscous drag, *Proc. 1974 Int. Conf. on Finite Element Methods in Engineering*, University of New South Wales, Australia, 661–676 (1974).
4. J. J. Russell, Equilibrium and stability of a whirling cable, Ph.D. Dissertation, the University of Michigan (1974).
5. V. V. Bolotin, *Nonconservative Problems of the Theory of Elastic Stability*, pp. 98–100. Pergamon Press, New York (1963).
6. D. T. Greenwood, *Principles of Dynamics*, pp. 367–369. Prentice-Hall, Englewood Cliffs, New Jersey (1965).

Résumé

On utilise un modèle de masse concentrée a deux degrés de liberté pour comprendre l'équlibre et la stabilité d'un câble tiré circulairement. Les cas particuliers considérés sont ceux sans trainée, avec trainée visqueuse et trainée visqueuse avec un vent transverse.

Zusammenfassung:

Ein Model mit Ersatzmassen und zwei Freiheitsgraden wird zur Untersuchung des Gleichgewichts und der Stabilität eines im Kreise gezogenen Kabels benutzt. Als besonders Fälle werden Ziehen ohne Widerstand, mit Reibungswiderstand und mit Reibungswiderstand unter Querwind behandelt.